A&A manuscript no.
(will be inserted by hand later)

Your thesaurus codes are:
16 (03.13.4 Methods: numerical; 02.18.7 Radiative transfer; 08.01.3 Stars: atmospheres; 02.12.1 Line: formation)

ASTRONOMY AND ASTROPHYSICS
July 27, 2001

Monte Carlo transition probabilities

L.B. Lucy

Astrophysics Group, Blackett Laboratory, Imperial College of Science, Technology and Medicine, Prince Consort Road, London SW7 2BW

Received ; accepted

Abstract. Transition probabilities governing the interaction of energy packets and matter are derived that allow Monte Carlo NLTE transfer codes to be constructed without simplifying the treatment of line formation. These probabilities are such that the Monte Carlo calculation asymptotically recovers the local emissivity of a gas in statistical and radiative equilibrium. Numerical experiments with one-point statistical equilibrium problems for Fe II and Hydrogen confirm this asymptotic behaviour. In addition, the resulting Monte Carlo emissivities are shown to be far less sensitive to errors in the populations the emitting levels than are the values obtained with the basic emissivity formula.

Key words: methods: numerical – radiative transfer – stars: atmospheres – Line: formation

1. Introduction

When Monte Carlo methods are used to compute the spectra of astronomical sources, it is advantageous to work with *indivisible*, monochromatic packets of radiant energy and to impose the constraint that when interacting with matter their energy is conserved in the co-moving frame. The first of these constraints leads to simple code and the second facilitates convergence to an accurate temperature stratification.

For a static atmosphere, the energy-conservation constraint automatically gives a divergence-free radiative flux even when the temperature stratification differs from the radiative equilibrium solution. A remarkable consequence is that the simple Λ-iteration device of adjusting the temperature to bring the matter into thermal equilibrium with the Monte Carlo radiation field results in rapid convergence to the close neighbourhood of the radiative equilibrium solution (Lucy 1999a). An especially notable aspect of this success is that this temperature-correction procedure is geometry-independent, and so these methods readily generalize to 2- and 3-D problems.

Send offprint requests to: L.B. Lucy

For an atmosphere in differential motion, the constraint that emitted and absorbed packets have the same co-moving energies yields a radiative flux that is rigorously divergence-free in every local matter frame. Determining the temperature stratification by bringing matter into thermal equilibrium with such a radiation field - i.e., by imposing radiative equilibrium in the co-moving frame - is an excellent approximation if the local cooling time scale is short compared to the local expansion time scale. This condition is well satisfied for the spectrum-forming layers of supernovae (SNe) and of stellar winds (Klein & Castor 1978).

The constraint that the energy packets be indivisible is advantageous from the point of view of coding simplicity. The interaction histories of the packets are then followed one-by-one as they propagate through the computational domain, with there being no necessity to return to any of a packet's interactions in order to continue or complete that interaction. This is to be contrasted with a Monte Carlo code that directly simulates physical processes by taking its quanta to be a sampling of the individual photons. Absorption of a Monte Carlo quantum is then often followed by the emission of several quanta as an atom cascades back to its ground state. Multiple returns to this interaction are then necessary in order to follow the subsequent paths of each of these cascade quanta. The resulting coding complexity is of course compounded by some of these quanta creating further cascades.

Although coding simplicity argues strongly in favour of indivisible packets, a counter argument is the apparent need to couple this constraint with an approximate treatment of line formation. Thus, in Monte Carlo codes for studying the dynamics of stellar winds (Abbott & Lucy 1985; Lucy & Abbott 1993) or for synthesizing the spectra of SNe (Lucy 1987; Mazzali & Lucy 1993), the integrity of the packets could readily be maintained because line formation was assumed to occur by coherent scattering in the matter frame. But significantly, an improved SN code has recently been described (Lucy 1999b) in which branching into the alternative downward transitions is properly taken into account without sacrificing indivisibility. Accordingly, an obvious question now is whether Monte

Carlo techniques can be developed that take full advantage of the coding simplicity that derives from energy-packet indivisibility without having to compromise the treatment of line formation. If this can be achieved, then, when combined with the energy-conserving constraint, Monte Carlo codes for computing general NLTE transfer problems become feasible.

2. Macro-atoms

As discussed in Sect. 1, it is common in Monte Carlo transfer codes to quantize radiation into monochromatic energy packets. But in such codes matter is not quantized, neither artificially into parcels of matter nor naturally into individual atoms. Instead, the continuum description of matter is retained, with macroscopic absorption and scattering coefficients governing the interaction histories of the energy packets.

Nevertheless, it now proves useful to imagine that matter is quantized into *macro-atoms* whose properties are such that their interactions with energy packets asymptotically reproduce the reprocessing of radiation by macroscopic volume elements of a gas that is in statistical and radiative equilibrium. But these macro-atoms, unlike energy packets, do not explicitly appear in the Monte Carlo code. As conceptual constructs, their utility is in facilitating the derivation and implementation of the Monte Carlo transition probabilities that result in an accurate treatment of line formation.

The general properties of macro-atoms are as follows:

1) Each macro-atom has discrete internal states in one-to-one correspondence with the energy levels of the atomic species being represented.

2) An inactive macro-atom can be activated to one of its internal states i by absorbing a packet of kinetic energy or a packet of radiant energy of an appropriate co-moving frequency.

3) An active macro-atom can undergo a transition from state i to any other state j without absorbing or emitting an energy packet.

4) An active macro-atom becomes inactive by emitting a packet of kinetic energy or a packet of radiant energy of an appropriate co-moving frequency.

5) The de-activating packet has the same energy in the macro-atom's frame as the original activating packet.

Figure 1 illustrates these general rules. An inactive macro-atom, with its internal discrete states shown schematically, encounters a packet of energy ϵ_0 and is activated to one of these states. The active macro-atom then undergoes two internal, radiationless transitions before deactivating itself by emitting a packet of energy ϵ_0.

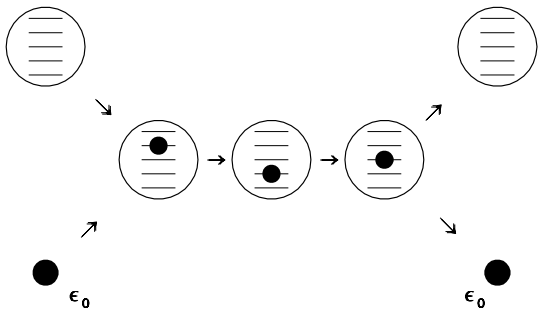

Fig. 1. Schematic representation of the interaction of a macro-atom with a packet of energy ϵ_0. The macro atom is activated by absorbing the energy packet, makes two radiationless transitions, and then de-activates by emitting a packet of energy ϵ_0.

3. Transition probabilities

In Sect. 2, the concept of a macro-atom was introduced by stating some general properties concerning its interaction with packets of kinetic or radiant energy. The challenge now is to derive explicit rules governing a macro-atom's activation, its subsequent internal transitions, and its eventual de-activation.

3.1. Basic equation

For the moment, we drop the notion of a macro-atom and consider a real atomic species in statistical equilibrium with the ambient conditions. Let ϵ_i denote the excitation *plus* ionization energy of level i and let R_{ij} denote the radiative rate for the transition $i \rightarrow j$. The rates per unit volume at which transitions into and out of i absorb and emit radiant energy are then

$$\dot{A}_i^R = R_{\ell i}\epsilon_{i\ell} \quad \textit{and} \quad \dot{E}_i^R = R_{i\ell}\epsilon_{i\ell} \quad , \tag{1}$$

respectively, where $\epsilon_{i\ell} = h\nu_{i\ell} = \epsilon_i - \epsilon_\ell$. Note the summation convention adopted for the suffix ℓ, which ranges over all levels $< i$, including those of lower ions. Similarly, below, the suffix u implies summation over all levels $> i$, including those of higher ions.

The corresponding rates at which kinetic energy is absorbed from, or contributed to the thermal pool by transitions to and from level i are

$$\dot{A}_i^C = C_{\ell i}\epsilon_{i\ell} \quad \textit{and} \quad \dot{E}_i^C = C_{i\ell}\epsilon_{i\ell} \quad , \tag{2}$$

where C_{ij} is the collisional rate per unit volume for the transition $i \rightarrow j$.

If we now define the total rate for the transition $i \rightarrow j$ to be $\mathcal{R}_{ij} = R_{ij} + C_{ij}$, then the net rate at which level i absorbs energy from the local environment is

$$\dot{A}_i^R + \dot{A}_i^C - \dot{E}_i^R - \dot{E}_i^C = (\mathcal{R}_{\ell i} - \mathcal{R}_{i\ell})\epsilon_{i\ell} \quad . \tag{3}$$

Eq.(3) is an identity obtained directly from the defining Eqs.(1) and (2). But we can transform it into a useful

equation by invoking our assumption of statistical equilibrium, which holds for level i if

$$(\mathcal{R}_{\ell i} - \mathcal{R}_{i\ell}) + (\mathcal{R}_{ui} - \mathcal{R}_{iu}) = 0 \quad . \tag{4}$$

This equation allows us to write the right-hand side of Eq.(3) as $-(\mathcal{R}_{ui} - \mathcal{R}_{iu})\epsilon_i - (\mathcal{R}_{\ell i} - \mathcal{R}_{i\ell})\epsilon_\ell$. Then, rearranging terms, we obtain the basic equation

$$\begin{aligned} &\dot{E}_i^R + \dot{E}_i^C + \mathcal{R}_{iu}\epsilon_i + \mathcal{R}_{i\ell}\epsilon_\ell \\ &= \dot{A}_i^R + \dot{A}_i^C + \mathcal{R}_{ui}\epsilon_i + \mathcal{R}_{\ell i}\epsilon_\ell \quad . \end{aligned} \tag{5}$$

When Eq.(5) is summed over all energy levels, the coupling terms cancel, giving

$$\sum_i (\dot{E}_i^R - \dot{A}_i^R) + \sum_i (\dot{E}_i^C - \dot{A}_i^C) = 0 \quad , \tag{6}$$

Thus, in statistical equilibrium, any inbalance between the emission and absorption of radiant energy by the atomic energy levels must be due to energy exchange with the thermal pool.

3.2. Interpretation

Eq.(5) expresses the fact that in statistical equilibrium the contribution from level i to the energy content of unit volume is stationary. In consequence, the net rate at which level i gains energy - the right-hand side of Eq.(5) - equals the net rate of loss - the left-hand side.

But the importance here of Eq.(5) lies in the various terms contributing to gains and losses by level i and their relevance for constucting transition rules for macro-atoms. The net rate of gain comprises the expected absorption terms $\dot{A}_i^R$ and $\dot{A}_i^C$ plus the terms $\mathcal{R}_{ui}\epsilon_i$ and $\mathcal{R}_{\ell i}\epsilon_\ell$ that clearly represent energy flows into i from upper and lower levels, respectively. Similarly, the net rate of loss comprises the expected emission terms $\dot{E}_i^R$ and $\dot{E}_i^C$ plus the terms $\mathcal{R}_{iu}\epsilon_i$ and $\mathcal{R}_{i\ell}\epsilon_\ell$ representing energy flows out of i to upper and lower levels.

The above remarks imply definitive values for the energy flows between level i and other levels. But this is not true. If Eq.(4) is rewritten in the form

$$\mathcal{R}_{iu} + \mathcal{R}_{i\ell} = \mathcal{R}_{ui} + \mathcal{R}_{\ell i} \quad , \tag{7}$$

then comparison with Eq.(5) shows immediately that an arbitrary quantity of energy ϵ may be added to ϵ_i and ϵ_ℓ without invalidating this equation. In doing this, we are of course merely shifting the zero point of the energy scale for excitation and ionization, which we are always free to do. Nevertheless, this freedom implies a corresponding indefiniteness in the magnitudes of the energy flow terms.

3.3. Stochastic interpretation

Notwithstanding this indefiniteness, we now interpret Eq.(5) in terms of macro-atoms absorbing and emitting energy packets and undergoing internal, radiationless transitions. In this interpretation, the terms $\dot{A}_i^R$ and $\dot{A}_i^C$ obviously represent the activation of macro-atoms to state i due to the absorption of packets of radiant and of kinetic energy, respectively.

Now consider an ensemble of active macro-atoms in state i. For this ensemble to reproduce the behaviour of the real system, the relative numbers of the macro-atoms that subsequently de-activate with the emission of a packet of radiant or kinetic energy or which make a radiationless transition to another state must be proportional to the relative values of the corresponding terms on the left-hand side of Eq.(5). Accordingly, for an individual macro-atom in state i, the probabilities that it de-activates with the emission of a packet of radiant or of kinetic energy are

$$p_i^R = \dot{E}_i^R/D_i \quad \textit{and} \quad p_i^C = \dot{E}_i^C/D_i \quad , \tag{8}$$

where

$$D_i = \dot{E}_i^R + \dot{E}_i^C + \mathcal{R}_{iu}\epsilon_i + \mathcal{R}_{i\ell}\epsilon_\ell \quad . \tag{9}$$

Similarly, the probabilities that it makes a radiationless transition to *particular* upper or lower states are

$$p_{iu} = \mathcal{R}_{iu}\epsilon_i/D_i \quad \textit{and} \quad p_{i\ell} = \mathcal{R}_{i\ell}\epsilon_\ell/D_i \quad . \tag{10}$$

Note that these transition probabilities depend not only on atomic data but also on ambient conditions. They are therefore functions of position.

4. Alternative formulations

Monte Carlo transition probabilities have been defined in Sect. 3 without guaranteeing their non-negativity. Of concern in this regard is stimulated emission when level populations are inverted. In anticipation of this issue, radiative rates were introduced without specifying whether for $i > j$ stimulated emission contributes positively to R_{ij} or negatively to R_{ji}.

4.1. General case

In the general case, inverted level populations may occur - i.e., $g_j n_i > g_i n_j$ for some $i > j$.

4.1.1. Definitions of rates

In order to avoid negative probabilities when levels are inverted, stimulated emissions must be added to spontaneous emissions and *not* treated as negative absorptions. Accordingly, for bound-bound (b-b) transitions, the radiative rates per unit volume are defined to be ($i > j$)

$$R_{ij} = (A_{ij} + B_{ij}\bar{J}_{ij}^e)n_i \quad \textit{and} \quad R_{ji} = B_{ji}\bar{J}_{ji}^a n_j \quad , \tag{11}$$

where $\bar{J}_{ij}^e$ and $\bar{J}_{ji}^a$ are the mean intensities averaged over the line's emission and absorption profiles, respectively -

see Mihalas (1978, p78). Similarly, for free-bound (f-b) and bound-free (b-f) transitions, we define

$$R_{\kappa i} = (\alpha_i^{sp} + \alpha_i^{st}) n_\kappa n_e \quad and \quad R_{i\kappa} = \gamma_i n_i \quad . \tag{12}$$

Here α_i^{sp} and α_i^{st} are the rate coefficients for spontaneous and stimulated recombinations to level i, respectively, while γ_i is the uncorrected rate coefficient for photoinizations from level i. Each of these three quantities can be expressed as an integral over frequency involving the b-f absorption coefficient for an atom excited to level i - see Mihalas (1978, pp130-131).

For collisions, a population inversion gives a negative rate if collisional de-excitations are treated as negative excitations. This is avoided by defining

$$C_{ij} = q_{ij} n_i n_e \quad and \quad C_{ji} = q_{ji} n_j n_e \quad . \tag{13}$$

With these expressions for the collisional and radiative rates, the probabilities defined by Eqs.(8) and (10) are non-negative provided only that the ϵ_i's are non-negative. This latter condition is satisfied with the standard convention that the ground state of the neutral atom has zero excitation energy.

4.1.2. Absorption of packets

Because $R_{\ell i}$ and therefore $\dot{A}_i^R$ are here defined without correcting for stimulated emission, the macroscopic line- and continuum-absorption coefficients that determine the flight paths of packets of radiant energy must also be defined without this correction. This ensures that the packets see a positive absorption coefficient even for a transition with a population inversion.

4.1.3. Emission of packets

If the Monte Carlo transition probabilities result in a macro-atom de-activating radiatively from state i, the next step is to detrmine the frequency of the photons comprising the emitted energy packet. First we suppose that i corresponds to a bound level.

Because $R_{i\ell}$ and therefore $\dot{E}_i^R$ here include stimulated emission, the process that radiatively de-activates the macro-atom may be either a spontaneous or a stimulated emission. The ratio of the probabilities of these alternatives is $\dot{E}_i^{sp} : \dot{E}_i^{st}$, where

$$\dot{E}_i^{sp} = A_{i\ell} n_i \epsilon_{i\ell} \quad and \quad \dot{E}_i^{st} = B_{i\ell} \bar{J}_{i\ell}^e n_i \epsilon_{i\ell} \tag{14}$$

are the contributions to $\dot{E}_i^R$ from spontaneous and stimulated emissions, respectively.

Having thus decided between spontaneous and stimulated emission, we must next choose a downward transition. For spontaneous line emission, the transition $i \rightarrow j$ is selected with probability $A_{ij} n_i \epsilon_{ij} / \dot{E}_i^{sp}$. For stimulated emission, on the other hand, the selection probability is $B_{ij} \bar{J}_{ij}^e n_i \epsilon_{ij} / \dot{E}_i^{st}$.

With the transition thus determined, the frequency of the emitted packet of radiant energy is selected by randomly sampling the line's emission profile. Efficient procedures for sampling standard profiles have been described by Lee (1974a,b).

Now we consider a macro-atom that de-activates from a continuum state κ. In this case, the probabilities of spontaneous and stimulated emission are in the ratio $\dot{E}_\kappa^{sp} : \dot{E}_\kappa^{st}$, where

$$\dot{E}_\kappa^{sp} = \alpha_{i\ell}^{sp} n_\kappa \epsilon_{\kappa\ell} \quad and \quad \dot{E}_\kappa^{st} = \alpha_{i\ell}^{ss} n_\kappa \epsilon_{\kappa\ell} \tag{15}$$

are the contributions to $\dot{E}_\kappa^R$ from spontaneous and stimulated emissions, respectively. The new frequency is then selected by randomly sampling the energy distribution of the spontaneous or the stimulated recombination continua.

4.1.4. Direction of propagation

If the above selection procedure rules that a packet of radiant energy is emitted spontaneously, then a new direction of propagation is chosen in accordance with this process's isotropic emission. On the other hand, for stimulated emission, the new direction of propagation is that of the stimulating photon. Thus, the new direction will be in solid angle $d\omega$ at θ, ϕ with probability $d\omega / 4\pi \times I_\nu(\theta,\phi)/J_\nu$, where ν is the frequency of the stimulating photon. Accordingly, a Monte Carlo code that treats stimulated emission separately must store a complete description of the radiation field - i.e., $I_\nu(\theta,\phi)$.

4.2. Standard case

For problems where population inversions are not anticipated, we can usefully make the traditional assumption that lines have identical emission and absorption profiles and treat stimulated emissions as negative absorptions - see Mihalas (1978, p78).

4.2.1. Definitions of rates

The radiative rates for b-b transitions are then $(i > j)$

$$R_{ij} = A_{ij} n_i \quad and \quad R_{ji} = (B_{ji} n_j - B_{ij} n_i) \bar{J}_{ji} \quad . \tag{16}$$

Similarly, for f-b and b-f transitions, we define

$$R_{\kappa i} = \alpha_i^{sp} n_\kappa n_e \quad and \quad R_{i\kappa} = \gamma_i^{corr} n_i \quad , \tag{17}$$

where the photionization coefficient is now corrected for stimulated recombinations.

For collisions, the absence of population inversions allows us the option of treating collisional de-excitations as negative excitations without the risk that Eqs.(8) and (10) will give negative probabilities. Accordingly, we now define

$$C_{ij} = 0 \quad and \quad C_{ji} = (q_{ji} n_j - q_{ij} n_i) n_e \tag{18}$$

This then implies that $\dot{E}_i^C$ and therefore also $p_i^C = 0$ for all i. Energy transfer from the radiation field to the thermal pool then occurs *explicitly* only via f-f absorptions.

4.2.2. Absorption of packets

Because $R_{\ell u}$ and therefore $\dot{A}_i^R$ are here defined with the correction for stimulated emission included, the macroscopic line and continuum absorption coefficients that determine flight paths must also include this correction. In the posited absence of population inversions, the packets still always see a positive absorption coefficient.

4.2.3. Emission of packets

Because $R_{i\ell}$ and therefore $\dot{E}_i^R$ now exclude stimulated emission, the process that radiatively de-activates a macro-atom is always a spontaneous emission. If i is a bound state, the frequency of the emitted packet is then decided as follows: the transition $i \rightarrow j$ is selected with probability $A_{ij} n_i \epsilon_{ij} / \dot{E}_i^R$, and then a frequency selected by randomly sampling this transition's emission profile.

For de-activation from a continuum state, the new frequency is selected by randomly sampling the energy distribution of the spontaneous recombination continua.

4.2.4. Direction of propagation

Because the de-activating process is in this case spontaneous emission, the new direction of propagation is selected according to isotropic emission. Thus, in contrast to the general case, we now do not need to know $I_\nu(\theta, \phi)$. In fact, from the Monte Carlo radiation field generated at one iteration, we only require the mean intensities J_ν. These allow us to compute transition probabilities from Eqs.(8) and (10) for use during the next iteration.

4.3. Large velocity gradients

The procedures described in Sects. 4.1 and 4.2 apply to both static and moving media. But for some important problems involving moving media, a substantial speeding up of the calculation with negligible loss of accuracy is possible by applying Sobolev's theory of line formation. In doing so, we take advantage of a small dimensionless quantity - the ratio of a line's Doppler width to the typical flow velocity, which implies an essentially constant velocity gradient over the zone in which a given pencil of radiation interacts with a particular line. The Monte Carlo codes for winds and SNe cited in Sect. 1 treat line formation in the Sobolev approximation.

The simplest case of this kind is that of homologous spherical expansion as is commonly assumed for SNe. This case will be treated here since it will be used in the test calculations of Sect. 5. Generalization to a spherically-symmetric stellar wind outflow is readily carried out by referring to Castor & Klein (1978). We also assume there are no population inversions and so treat stimulated emissions as negative absorptions as in Sect. 4.2.

4.3.1. Definitions of rates

The radiative rates for b-b transitions are then

$$R_{ij} = A_{ij} \beta_{ji} n_i \quad and \quad R_{ji} = (B_{ji} n_j - B_{ij} n_i) \beta_{ji} J_{ji}^b \quad . \tag{19}$$

Here J_{ji}^b is the mean intensity at the far blue wing of the transition $j \rightarrow i$, and β_{ij} is the Sobolev escape probability for this transition, given by

$$\beta_{ji} = \frac{1}{\tau_{ji}} [1 - \exp(-\tau_{ji})] \quad , \tag{20}$$

where τ_{ji}, the transition's Sobolev optical depth, is

$$\tau_{ji} = (B_{ji} n_j - B_{ij} n_i) \frac{hct_E}{4\pi} \quad , \tag{21}$$

with t_E being the elapsed time since the SN exploded. For f-b and b-f transitions, the rates are as in Eq.(17). For collisions, the rates are as in Eq.(18).

4.3.2. Absorption of packets

The absorption of packets by lines is determined by the Sobolev optical depths given by Eq.(21). Absorption of a packet to the continuum is determined by the conventional macroscopic absorption coefficient corrected for stimulated emission.

4.3.3. Emission of packets

The frequency of an emitted packet of radiant energy is decided as follows: for de-activation from a bound state i, the transition $i \rightarrow j$ is selected with probability $A_{ij} \beta_{ji} n_i \epsilon_{ij} / \dot{E}_i^R$, where $\dot{E}_i^R$ is evaluated with Eq.(1) using the decay rates from Eq.(19). For de-activation from a continuum state, the new frequency is, as in Sect. 4.2.3, selected by randomly sampling the energy distribution of the spontaneous recombination continua.

4.3.4. Direction of propagation

If a packet is emitted from a continuum state, the new direction of propagation is selected according to isotropic emission since the emission in this case is spontaneous. For de-activation from a bound state, the emission is also isotropic since there is no kinematically-preferred direction for homologous spherical expansion. This is not true for a stellar wind.

5. Convergence tests

The Monte Carlo transition probabilities derived in Sect. 3 are designed to reproduce asymptotically the local reprocessing of radiation that occurs in an atmosphere where

the atomic species are in statistical equilibrium with the ambient conditions and for which radiative equilibrium in the matter frame holds. This would seem to imply that, to test these probabilities, we must first solve a NLTE atmosphere problem with a conventional code and then attempt to recover the local reprocessing with this Monte Carlo machinary. But fortunately, simpler and more rigorous tests are possible if we note from Eq.(6) that, in the absence of coupling to the thermal pool, statistical equilibrium implies radiative equilibrium in the matter frame. Accordingly, we now carry out one-point tests with collisional terms excluded.

5.1. Fe II

As a first test, the Monte Carlo transition probabilities are applied to the model Fe II ion with $N = 394$ levels used previously (Lucy 1999b) to investigate the accuracy of approximate treatments of line formation in SNe envelopes. The energy levels of the Fe II ion and the f-values for permitted transitions were extracted from the Kurucz–Bell (1995) compilation by M.Lennon (Munich). Einstein A-values for forbidden transitions are from Quinet et al.(1996) and Nussbaumer & Storey (1988). Collision strengths, which are needed in Sect.7, are from Zhang & Pradhan (1995) and van Regemorter (1962).

As previously, the ambient radiation field determining the quantities J^b_{ji} in Eq.(19) is taken to be $WB_\nu(T_b)$ with $T_b = 12500K$ and dilution factor $W = 0.5$, corresponding to $r = R$. The density parameter is $n(FeII) = 6.6 \times 10^7 cm^{-3}$, while the time since explosion is $t_E = 13\,days$. With these parameters specified, this one-point statistical equilibrium problem - Eq.(4) for $N-1$ levels plus a normalization constraint - is non-linear in the unknowns n_i because the rate coefficients in Eq.(19) depend on the n_i through the Sobolev escape probabilities. But simple repeated back substitutions give a highly accurate solution $n_i^{(x)}$ in ~ 10 iterations.

5.1.1. Monte Carlo experiment

With $n_i^{(x)}$ thus determined, the Fe II level emissivites $\dot{E}_i^R$ and absorption rates $\dot{A}_i^R$ can be computed from Eq.(1). We now test the Monte Carlo transition probabilities by seeing how accurately they reproduce these values $\dot{E}_i^R$. Note that it is sufficient to test *level* emissivities since if these are exact so also are the line emissivities computed as described in Sect. 4.3.3.

In the following Monte Carlo experiment, $\mathcal{N}$ packets of radiant energy are absorbed and subsequently emitted by a macro-atom representing a macroscopic volume element of Fe II ions in the ambient conditions specified above. The energies of these packets are taken to be equal and given by $\epsilon_0 = \dot{A}^R/\mathcal{N}$, where $\dot{A}^R = \sum_i \dot{A}_i^R$. The calculation proceeds step-by-step as follows:

1) $\mathcal{N}_i = \mathcal{N}\dot{A}_i^R/\dot{A}^R$ of the packets activate the macro-atom to internal state i.

2) The transition probabilities p_i^R, p_{iu} and $p_{i\ell}$ for a macro-atom in state i are computed from Eqs.(8) and (10).

3) The transition probabilities sum to one, and so each corresponds to a segment (x_k, x_{k+1}) of the interval (0,1). A particular transition is therefore selected by computing a random number x in (0,1) and finding in which segment it falls.

4) If the selected transition is the de-activation of the macro-atom, we update $\dot{E}_i^{MC}$ to $\dot{E}_i^{MC} + \epsilon_0$ and then return to step 3) to process the next activation of state i, or to step 2) to process the first of the packets that activate the macro-atom to state $i+1$.

5) If the selected transition is an internal transition to state j, then we return to step 2) with j replacing i.

6) When all $\mathcal{N}$ packets have been processed in this way, the final elements of the vector $\dot{E}_i^{MC}$ are our estimates of the level emissivities $\dot{E}_i^R$

5.1.2. Results of experiment

As a single measure of the accuracy of the estimated level emissivities, we compute the quantity

$$\delta = \sum_i |\dot{E}_i^{MC} - \dot{E}_i^R| \,/\, \sum_i \dot{E}_i^R \quad . \tag{22}$$

This is the mean of the absolute fractional errors of the $\dot{E}_i^{MC}$ when weighted by $\dot{E}_i^R$.

Figure 2 shows the values of δ, expressed as percentage errors, found in a series of trials with $\mathcal{N}$ increasing from 10^4 to 10^7. The values of δ decrease monotonically with increasing $\mathcal{N}$, falling to 0.36 percent for $\mathcal{N} = 10^7$. More importantly, the errors accurately follow an $\mathcal{N}^{-1/2}$ line, as expected if the only source of error is the sampling error associated with step 3) of the Monte Carlo experiments. This strongly suggests that asymptotically macro-atoms obeying the transition probabilities developed in Sect. 3 do indeed exactly reproduce the reprocessing of radiation by macroscopic volume elements.

Also included in Fig.2 are values of δ obtained when the transition probabilities are computed using values of the energy levels ϵ_i increased by 5eV. This is to investigate the consequences of the dependence of the energy flow terms in Eq.(5) - and therefore also of the transition probabilities - on the zero point of the scale of excitation energy. These results also track an $\mathcal{N}^{-1/2}$ line and so indicate that the predicted line emissivities are asymptotically independent of the zero point. But since the open circles are marginally higher, there is an indication that increasing the zero point gives slighty less accurate level emissivities at a given $\mathcal{N}$.

In the Monte Carlo codes for stellar winds and SNe cited in Sect. 1, line formation is treated approximately, assuming either resonant scattering or downward branching following absorption. For both assumptions,

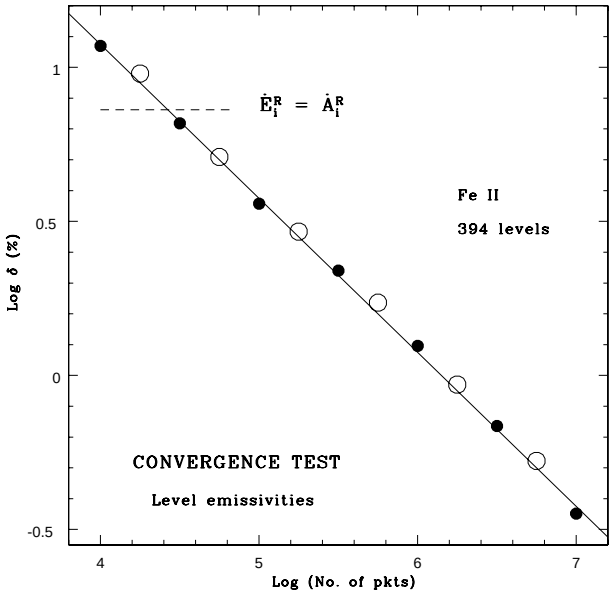

Fig. 2. Convergence test. The mean error δ defined by Eq.(22) is plotted against $\mathcal{N}$, the number of packets in the Monte Carlo experiment. The open circles refer to the case where excitation energies are increased by 5eV. The straight line drawn by eye has slope $= -0.5$. Also indicated is the mean error when the level emissivities are assumed equal to the level absorption rates.

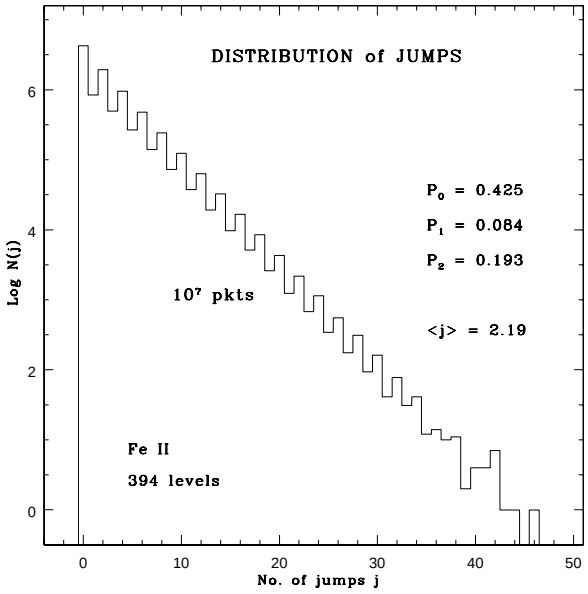

Fig. 3. Histogram of $N(j)$, the number of times in an experiment with $\mathcal{N} = 10^7$ that the macro-atom underwent j internal transitions - or jumps - before de-activating with the emission of an energy packet. The mean number of jumps $< j >$ and the probabilities of de-activation after $j = 0 - 2$ jumps are indicated.

$\dot{E}_i^R = \dot{A}_i^R$, corresponding to a macro-atom for which de-activation always immediately follows activation - i.e., $p_i^R = 1$ for all i. In this case, as indicated on Fig.2, $\delta = 7.28$ percent. Thus, when the points in Fig.2 drop below this value, the success must be due to the internal, radiationless transitions governed by the probabilities p_{iu} and $p_{i\ell}$.

5.1.3. Distribution of jumps

The above experiments show that despite the complexity of its level structure the Fe II ion's reprocessing of radiation is accurately simulated by the Monte Carlo transition probabilities. But from a computational standpoint, a concern is just how many of the internal transitions - or jumps - are required to achieve this. To answer this, the number of jumps before de-activation was recorded for each absorbed packet in the above $\mathcal{N} = 10^7$ trial and used to derive $N(j)$, the number of packets requiring j jumps.

From the histogram $N(j)$, we find that the expected number of jumps is $< j >= 2.19$ and that the probability of immediate de-activation - i.e., zero jumps - is $P_0 = 0.425$. Evidently, fears of numerous, time- consuming internal transitions are ill-founded.

Figure 3 is a logarithmic plot of $N(j)$. This reveals a power-law decline with increasing j but with alternating deviations indicating that an even number of jumps before de-activation is favoured. A simple model suggests the origin of this curious behaviour. Consider a 3-level atom with $\epsilon_3 > \epsilon_2 > \epsilon_1 = 0$ and suppose that level 2 is metastable with $A_{21} = 0$. Because $B_{12} = 0$, the macro-atom can only be activated to state 3 and, because $A_{21} = B_{21} = 0$, the macro-atom cannot de-activate from state 2. Moreover, because $\epsilon_1 = 0$, Eq.(10) gives $p_{31} = p_{21} = 0$, and so state 1 of the macro-atom cannot be reached. Accordingly, following activation at state 3, the macro-atom de-activates with probability p or jumps to state 2 with probability $1 - p$, from whence it returns to state 3 with probability $p_{23} = 1$. It is now simple to prove that the probabilty of j jumps before de-activation is $P_j = p(1-p)^{j/2}$ if j is even, and $P_j = 0$ if j is odd. The Fe II ion's numerous low-lying metastable levels are presumably playing the role of level 2 and thereby favouring an even number of jumps.

Histograms $N(j)$ have also been computed for two other cases. First, the above trial was repeated with the ϵ_i's increased by 5eV as in Sect. 5.1.2. This change increases $< j >$ - to 4.54 - as expected since the probabilities p_{iu} and $p_{i\ell}$ are thereby increased and p_i^R correspondingly decreased. Evidently, the standard choice of energy-level zero point leads to the most computationally-efficient set of Monte Carlo transition probabilities.

In the second case, W is decreased from 0.5 to 0.067, corresponding to $r = 2R$. This change decreases $< j >$ - from 2.19 to 1.29 - as expected given the weakening of the radiative excitation rates.

5.2. Hydrogen

Although the Fe II case suffices to demonstrate the validity of the Monte Carlo transition probabilities, a test including b-f and f-b transitions is perhaps of interest. Accordingly, the above test at one point in a SN's envelope has also been carried out for a 15-level model of the H atom, with level 15 being the continuum κ. The 14 bound levels correspond to principal quantum numbers $n = 1-14$, with each level having consolidated statistical weight $g = 2n^2$.

As in the Fe II case, the ambient radiation field incident on the blue wings of the b-b transitions is $WB_\nu(T_b)$, but now with $T_b = 6000K$ and $W = 0.067$. Beyond the Lyman limit, we assume zero intensity, so that photoionizations occur only from excited states. Correspondingly, recombinations to $n = 1$ are excluded on the assumption of immediate photoionization. The density parameter is $N(H) = 1.88 \times 10^9 cm^{-3}$, the electron temperature $T_e = 4800K$, and the time since explosion $t_E = 10\,days$. With parameters specified, this non-linear statistical equilibrium problem can be solved with repeated back substitutions, giving a highly accurate solution $n_i^{(x)}$ in $\sim$ 30 iterations.

With $n_i^{(x)}$ determined, Monte Carlo experiments as described in Sect. 5.1.1 can be carried out to test if level emissivities can also be recovered in this case. Two such trials, with $\mathcal{N} = 10^4$ and 10^5, are compared with the accurate solution in Fig.4. The results show excellent agreement for $\mathcal{N} = 10^5$. Note in particular the success with $\dot{E}_\kappa^R$, which is the rate of ionization energy loss due to recombinations, and with $\dot{E}_2^R$, whose very low value is due to the strong trapping of $L\alpha$ photons.

5.3. Alternative test of convergence

Thus far in this section, a Monte Carlo procedure has been used to validate the Monte Carlo transition probabilities developed in Sect.3. This has the advantage of following closely and therefore illustrating their use in realistic NLTE calculations. But for feasible values of $\mathcal{N}$, sampling errors limit the accuracy of such tests.

In order to test to higher precision, approximate level emissivities $\dot{E}_i^{(m)}$ can be computed recursively according to the following scheme:

$$\dot{E}_i^{(m)} = p_i^R \sum_{r=1}^{m} G_i^{(r)} \quad , \tag{23}$$

where p_i^R is the radiative de-activation probability from Eq.(9) and $G_i^{(r)}$ is the increment at cycle r to the summation approximating the rate at which level i gains energy - i.e. the right-hand side of Eq.(5). This increment is derived from the previous increment by applying the transition probabilities from Eq.(10). Thus

$$G_i^{(r)} = \sum_j p_{ji} G_j^{(r-1)} \quad , \tag{24}$$

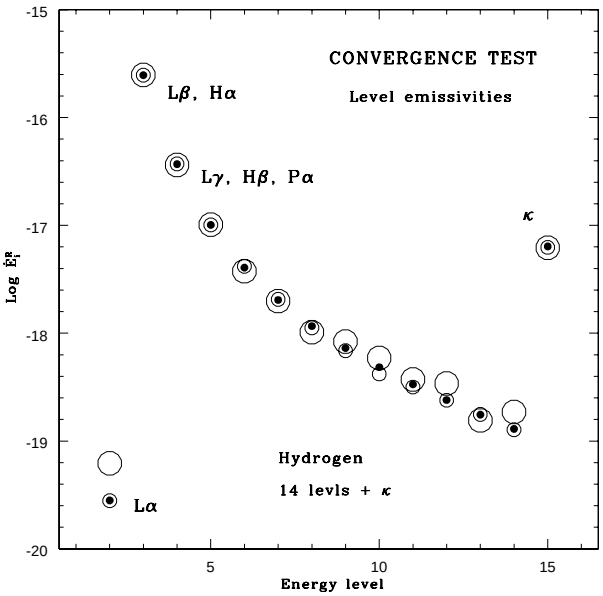

Fig. 4. Level emissivities (cgs) for Hydrogen. Results for trials with $\mathcal{N} = 10^4$ (large open circles) and $\mathcal{N} = 10^5$ (small open circles) are compared with exact values (filled circles). The lines contributing to the level emissivities are indicated for $n = 2-4$.

and the recursion cycles are initiated by setting

$$G_i^{(1)} = \dot{A}_i^R \quad . \tag{25}$$

As with the Monte Carlo experiment, the accuracy of the vectors $\dot{E}_i^{(m)}$ are measured by computing δ defined by Eq.(22). For $m = 17$, δ drops below the value 0.36 percent found in Sect.5.1.2 with $\mathcal{N} = 10^7$ - see Fig.2. As the recursion procedure continues further, δ decreases monotonically until at $m \simeq 60$ it drops to a value of $\simeq 10^{-8}$, at which point machine precision or accumulated roundoff errors halt further progress. This test clearly confirms and strengthens the earlier test of the Monte Carlo transition probabilities.

6. Sensitivity experiment

Because packets conserve energy on interaction with matter, the Monte Carlo radiation field has divergence-free flux, a result that is completely insensitive to the temperature stratification and which facilitates rapid convergence to the radiative equilibrium solution (Sect. 1). Now, having retained this divergence-free property while adding an asymptotically-correct reprocessing of radiation for matter in statistical and thermal equilibrium, we investigate the sensitivity of this reprocessing to departures from statistical equilibrium. If the reprocessing is insensitive, we can plausibly anticipate good covergence characteristics when this Monte Carlo procedure is used to solve NLTE problems.

The sensitivity test is simply a repetition of the Fe II experiment of Sect. 5.1.1, but now $n_i^{(x)}$ is replaced by

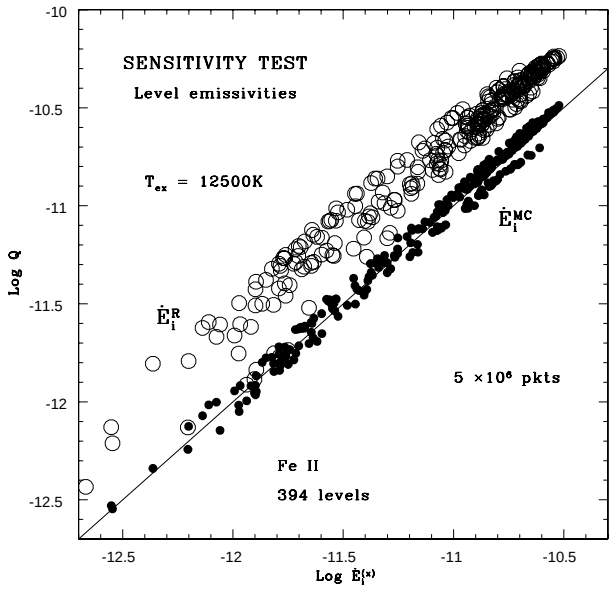

Fig. 5. Sensitivity test. For a Boltzmann distribution over excited states at $T_{ex} = 12500K$, the level emissivities (cgs) obtained with the Monte Carlo transition probabilities (filled circles) and with the basic formula (open circles) are plotted against the exact emissivities obtained with $n_i^{(x)}$. The Mont Carlo emissivities derive from a trial with $\mathcal{N} = 5 \times 10^6$ packets.

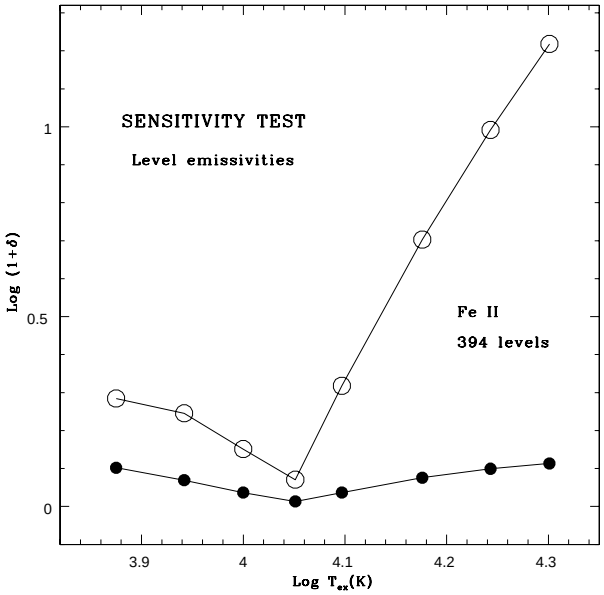

Fig. 6. Sensitivity test. Logarithmic errors of the emissivity vectors $\dot{E}_i^{MC}$ and $\dot{E}_i^R$ evaluated for Boltzmann distributions over excited states plotted against T_{ex}. The Monte Carlo emissivities derive from trials with $\mathcal{N} = 5 \times 10^6$ packets.

the Boltzmann distribution at excitation temperature T_{ex}. Because complete insensitivity cannot be expected, it is instructive to compare the level emissivities $\dot{E}_i^{MC}$ obtained when $n_i \neq n_i^{(x)}$ with the corresponding values $\dot{E}_i^R$ predicted by Eq.(1) with decay rates from Eq.(19). This latter calculation represents exactly the standard approach in which the radiation field is computed from the Radiative Transfer Eq. (RTE), with emissivity coefficient evaluated using the current estimates of level populations.

In Fig.5, the quantities $\dot{E}_i^{MC}$ and $\dot{E}_i^R$ obtained with $T_{ex} = 12500K$ are plotted against $\dot{E}_i^{(x)}$, the level emissivities when $n_i = n_i^{(x)}$. This Monte Carlo trial and those below have $\mathcal{N} = 5 \times 10^6$ packets, so sampling errors (cf. Fig.2) contribute negligibly to the scatter of the $\dot{E}_i^{MC}$ values.

Figure 5 shows that, in this particular case, the Monte Carlo level emissivities are far less sensitive to the departure of n_i from $n_i^{(x)}$ than are the emissivities computed directly from the basic formula. For the most part, the $\dot{E}_i^{MC}$ are in error by < 0.1 dex, with little evidence of bias, while the $\dot{E}_i^R$ are systematically offset by $\sim +0.3$ dex.

To show that this insensitivity is in fact a rather general property of the Monte Carlo procedure, the above test is repeated with T_{ex} ranging from $7500K$ to $20000K$ and the resulting mean errors defined by Eq.(22) are plotted in Fig.6. From this plot, we see that $\dot{E}_i^R$ gives reasonably accurate emissivities - errors $\lesssim 0.1$ dex - only in the immediate neighbourhood of the minimum at $T_{ex} = 11250K$. On the other hand, the values $\dot{E}_i^{MC}$ meet this criterion across this entire range.

For $\dot{E}_i^R$, the strong sensitivity to T_{ex} is readily understood. Because the sum $R_{i\ell}\epsilon_{i\ell} \propto n_i$, errors in the level populations directly translate into errors in $\dot{E}_i^R$.

Now consider the sensitivity of $\dot{E}_i^{MC}$. This quantity is determined by the rate at which active macro-atoms reach state i, and this happens by direct absorptions of packets into this state or by transitions from other states. Either way, the accuracy of the source vectors $\dot{A}_i^R$ and $\dot{A}_i^C$ is clearly fundamental to the accuracy of the vector $\dot{E}_i^{MC}$. But the dominant contributors to the elements of these source vectors - see Eqs.(1) and (2) - are transitions from the ground state and from low-lying metastable levels, and the estimated populations of these levels are unlikely to be seriously in error. In particular, with an assumed Boltzmann distribution over excited states, the n_i of these low levels is insensitive to T_{ex} and do not differ much from $n_i^{(x)}$. In contrast, the populations of high levels are quite likely to be badly estimated and are acutely sensitive to T_{ex}.

The likely beneficial impact of this insensitivity on the iterations needed to derive NLTE solutions is worth stressing. With the conventional RTE approach, an erroneously overpopulated upper level i pollutes the radiation field with spurious line photons at frequencies ν_{ij} $(j < i)$, and these are sources of excitation for level i when level populations are next solved for. To some degree therefore such an error is *self-sustaining* and so is not rapidly eliminated. This effect contributes to the slow convergence typical of

NLTE codes. In contrast, with the Monte Carlo approach, this pollution does not happen and so for a sufficiently large $\mathcal{N}$) a high quality radiation field is obtained immediately provided that the initial populations of the low-lying levels are estimated sensibly.

7. Departures from radiative equilibrium

The Monte Carlo transition probabilities have been developed to meet the challenge of solving simultaneously for statistical and radiative equilibrium for 2- and 3-D problems. Less challenging technically are problems where the constraint of radiative equilibrium is not appropriate. Such problems arise, for example, in stellar chromospheres and coronae where some ill-understood heating mechanism raises the gas temperature well above that of the photosphere. This results in the collisional creation of UV and optical photons that provide spectroscopic diagnostics of the temperature stratification in such zones and therefore also that of the heating mechanism.

Inspection of Eqs.(5) and (6) strongly suggests that the Monte Carlo transition probabilities should also asymptotically reproduce the emissivity of a gas where the photons derive from collisional excitation via the A_i^C term. As before, this can be tested with a one-point statistical equilibrium calculation. Accordingly, the Fe II test problem of Sect. 5.1 is repeated but now with collisional terms included and with the ambient radiation field assigned zero intensity. In this problem, therefore, all photons emitted by the Fe II levels originate from collisional excitation. This is to be contrasted with the previous tests where collisional terms were excluded.

The only parameters of this test are the electron temperature and density, and these are assigned the values $T_e = 2 \times 10^4 K$ and $N_e = 10^8 cm^{-3}$. The resulting one-point statical equilibrium problem is linear and so solved without iteration. From this solution, accurate values of the level emissivities $\dot{E}_i^R$ are computed from Eq.(1).

The next step is to derive Monte Carlo estimates of the level estimates by carrying out the Monte Carlo experiment of Sect.5.1.1. The only changes needed are the following: since the solution has population inversions the general formulation of Sect. 4.1 must be adopted to avoid negative probabilities. Secondly, since in this test a macro-atom is always activated by a packet of kinetic energy, the energy of these packets is taken to be $\epsilon_0 = \dot{A}^C/\mathcal{N}$, where $\dot{A}^C = \sum_i \dot{A}_i^C$. Correspondingly, at step (1) of the experiment, $\mathcal{N}_i = \mathcal{N}\dot{A}_i^C/\dot{A}^C$.

Apart from these changes, the convergence experiment proceeds as in Sects. 5.1.1 and 5.1.2. The result is a plot similar to Fig.2, with $\delta = 0.19$ percent for $\mathcal{N} = 10^7$. Thus the Monte Carlo transition probabilities are indeed applicable to problems where some non-radiative energy transfer mechanism creates a radiation field that is not in radiative equilibrium. The advantage of treating such problems with this technique are the coding simplicity that results from indivisible energy packets and the possibility of treating 2- and 3-D problems.

8. Conclusion

The limited aim of this paper has been to see if Monte Carlo transfer codes whose quanta are indestructable energy packets can be constructed without resorting to simplified treatments of line formation. To this end, the concept of a macro-atom has been introduced and rules established governing its activation and de-activation as well as its transitions between internal states. These rules - the Monte Carlo transition probabilities - have been derived by demanding that the macro-atom's emission of energy packets asymptotically reproduces the local emissivity of a gas in statistical and radiative equilibrium; and these rules' validity has been confirmed with one-point test problems.

Evidently, the next step is to implement these transition probabilities in a code to solve a realistic NLTE problem for a stratified medium and thus to investigate the practicality of this technique for problems of current interest. In a companion paper, a Monte Carlo NLTE code treating the formation of H lines in a Type II SN envelope will be described and used to illustrate the convergence behaviour of iterations to obtain both the level populations and the temperature stratification.

Acknowledgements. The work described in Sect.7 was carried out following questions raised by C.Jordan.

References

Abbott D.C., Lucy L.B. 1985, ApJ 288, 679
Klein R.I., Castor J.I. 1978, ApJ 220,902
Kurucz R.L., Bell B., 1995, Kurucz CD-ROM No. 23
Lee J.-S. 1974a, ApJ 187, 159
Lee J.-S. 1974b, ApJ 192, 465
Lucy L.B., 1987, In: Danziger I.J. (ed.) ESO Workshop on SN 1987A, p. 417
Lucy L.B. 1999a, A&A 344, 282
Lucy L.B. 1999b, A&A 345, 211
Lucy L.B., Abbott D.C. 1993, ApJ 405, 738
Mazzali P.A., Lucy L.B. 1993, A&A 279, 447
Mihalas D., 1978, Stellar Atmospheres (2nd ed.). W.H.Freeman & Co., San Francisco
Nussbaumer H., Storey P.J. 1988, A&A 193, 327
Quinet P., Le Dourneuf M., Zeippen C.J. 1996, A&AS 120, 361
van Regemorter H. 1962, ApJ 136, 906
Zhang H.L., Pradhan A.K. 1995, A&A 293, 953